Journal of Applied Electrochemistry

Electrochemical characterization of biodeterioration of paint films containing cadmium yellow pigment

--Manuscript Draft--

Manuscript Number:	
Full Title:	Electrochemical characterization of biodeterioration of paint films containing cadmium yellow pigment
Article Type:	Manuscript
Keywords:	Electrochemistry; Biodeterioration, Cadmium sulfide, Egg tempera; egg-oil emulsion; FTIR.
Corresponding Author:	Antonio Domenech-Carbo, PhD University of Valencia Burjassot, Valencia SPAIN
Corresponding Author Secondary Information:	
Corresponding Author's Institution:	University of Valencia
Corresponding Author's Secondary Institution:	
First Author:	Antonio Domenech-Carbo, PhD
First Author Secondary Information:	
Order of Authors:	Antonio Domenech-Carbo, PhD
	Annette S Ortiz-Miranda, PhD
	María Teresa Doménech-Carbó, PhD
	Laura Osete-Cortina, PhD
	Francisco Manuel Valle-Algarra, PhD
	Fernando Bolívar-Galiano, PhD
	Inés Martín-Sánchez, PhD
	María del Mar López-Miras, PhD
Order of Authors Secondary Information:	
Funding Information:	MINECO (CTQ2014-53736-C3-2-P) — Prof. Antonio Domenech-Carbo
	MINECO (CTQ2014-53736-C3-1-P) — Prof. María Teresa Doménech-Carbó
Abstract:	The voltammetry of microparticles (VMP) methodology was used to characterize the biological attack of different bacteria and fungi to reconstructed egg tempera and egg-linseed oil emulsion paint films containing cadmium yellow (CdS), which mimic historical painting techniques. When these paint films are in contact with aqueous acetate buffer, different cathodic signals are observed. As result of the crossing of VMP data with attenuated total reflectance Fourier transform infrared spectroscopy (ATR-FTIR), scanning electrochemical microscopy (SECM), field emission scanning electron microscopy (FESEM) and atomic force microscopy (AFM), these voltammetric signals can be associated with the reduction of CdS and different complexes associated to the proteinaceous and fatty acid fractions of the binders. After biological attack with different fungi (Acremonium crhysogenum, Aspergillus niger, Mucor roxii, Penicillium chrysogenum, and Trichoderma pseudokoningii) and bacteria (Arthrobacter oxydans, Bacillus amyloliquefaciens, and Streptomyces cellulofans) the observed electrochemical signals experience specific modifications depending on the binder and the biological agent, allowing for an electrochemical monitoring of biological attack.

Suggested Reviewers:	Fritz Scholz, PhD Professor, E.-M.-Arndt-Universität Greifswald fscholz@uni-greifswald.de Expertise in solid state electrochemistry; developer of the voltammetry of microparticles methodology
	Juergen Heinze, PhD Professor, Universität Freiburg juergen.heinze@physchem.uni-freiburg.de Expertise in solid state electrochemistry
	Annemie Adriaens, PhD Professor, Inflammatie-researchcentrum annemie.adriaens@ugent.be Expertise in electroanalytical methods applied to conservation of cultural heritage
	Frank Marken, PhD Professor, Bath Spa University f.marken@bath.ac.uk Expertise in solid state electrochemistry
	Howell G.M. Edwards, PhD Professor, University of Pittsburgh Bradford H.G.M.Edwards@Bradford.ac.uk Expertise in Raman and infrared spectroscopies applied to cultural heritage

Electrochemical characterization of biodeterioration of paint films containing cadmium yellow pigment

Annette S. Ortiz-Miranda[a], Antonio Doménech-Carbó*[b], María Teresa Doménech-Carbó[a], Laura Osete-Cortina[a], Francisco M. Valle-Algarra[b], Fernando Bolívar-Galiano[c], Inés Martín-Sánchez[d], María del Mar López-Miras[c]

[a]: Institut de Restauració del Patrimoni. Universitat Politècnica de València. Camí de Vera 14, 46022, València, Spain.
[b]: Departament de Química Analítica. Universitat de València. Dr. Moliner, 50, 46100 Burjassot (València) Spain.
[c]: Departamento de Pintura. Universidad de Granada. (Spain)
[d]: Departamento de Microbiología, Universidad de Granada (Spain).

* Corresponding author. E-mail: antonio.domenech@uv.es

Keywords: Electrochemistry; Biodeterioration, Cadmium sulfide, Egg tempera; egg-oil emulsion; FTIR.

Abstract

The voltammetry of microparticles (VMP) methodology was used to characterize the biological attack of different bacteria and fungi to reconstructed egg tempera and egg-linseed oil emulsion paint films containing cadmium yellow (CdS), which mimic historical painting techniques. When these paint films are in contact with aqueous acetate buffer, different cathodic signals are observed. As result of the crossing of VMP data with attenuated total reflectance Fourier transform infrared spectroscopy (ATR-FTIR), scanning electrochemical microscopy (SECM), field emission scanning electron microscopy (FESEM) and atomic force microscopy (AFM), these voltammetric signals can be associated with the reduction of CdS and different complexes associated to the proteinaceous and fatty acid fractions of the binders. After biological attack with different fungi (*Acremonium crhysogenum*, *Aspergillus niger*, *Mucor roxii*, *Penicillium chrysogenum*, and *Trichoderma pseudokoningii*) and bacteria (*Arthrobacter oxydans*, *Bacillus amyloliquefaciens*, and *Streptomyces cellulofans*) the observed electrochemical signals experience specific modifications depending on the binder and the biological agent, allowing for an electrochemical monitoring of biological attack.

1. Introduction

Biodeterioration is a problem affecting paintings which is of crucial importance in the conservation of works of art. In the last decades, studies in the field of conservation of heritage on this subject are, in general, focused on the direct isolation and identification of the microbiological agents that act on the different components of the painting [1-3]. Attempts to correlate microbial growth with type of materials present in paintings have been made by placing pieces of painting prepared with different supports and binding media on suitable culture media further inoculated with microorganisms and incubated under laboratory conditions so that the extent of the microbial colonization could be evaluated [4]. An alternative strategy consisted of preparing mock paintings prepared according to the traditional recipes that are exposed to soil for promoting colonization by bacteria and fungi that were isolated, identified and used for re-infecting sterile mock paintings in order to determine their ability for colonizing paintings [5]. These studies have demonstrated that the composition of the different parts of the painting (support, ground and paint layers) is determinant when the artwork undergoes a microbial attack. Type of support (canvas or panel) and binding medium (oil paints, temper or watercolours) mainly determines the selective growing of microorganisms [6]. A wide range of species have been identified as potential colonizing agents of paintings. Among them, *Alternaria*, *Aspergillus*, *Aureobasidium*, *Chaetomium*, *Cladosporium*, *Eurotium*, *Fusarium*, *Mucor*, *Cephalosporium (Acremonium)*, *Penicillium* and *Spicaria* fungi and *Bacillus*, *Arthrobacter*, *Acinetobacter*, *Stenotrophomonas* and *Delftia* bacteria [3,7,8].

Characterization of the damaging effects produced by these microbial agents has also been the aim of many studies, specially those affecting the organic compounds composing the support and the binding media [9]. These materials provide excellent substrates for the growth of microorganisms, in particular, fungi and most bacteria. It has been shown that the microorganism colonization in canvas painting starts in the organic materials present on the reverse side where the cellulosic support and proteinaceous binders present in the support. Sometimes, the chalk-rich ground can act as substrate for microbial growing [6]. The binding media present in the obverse side of the painting are susceptible to attack by transient airborne microorganisms such as bacteria and fungi which can accumulate on the painted surface for a long time as

spores. Their further growth can result in the detachment of the paint layer from the support especially in conditions of high humidity [10]. Spots due to colored metabolic byproducts excreted by the microorganisms have also been frequently observed [11]. Laboratory experiments have demonstrated that α-aminobutyric acid in combination with L-malic acid and glucose are the main products responsible for the fox spots [12-14]. Fungal amino acids, metabolic acids, sugars and lipids and their breakdown products (fatty acids, glycerol) have also been found in fox spots. In these cases, the interaction of amino acids and sugars results in melanoidin, a colored substance, by a Maillard browning reaction. Fading of the paint layer is other degradation effect caused by the growth of bacteria and fungi in the paintings [11,15].

Changes caused in the structure of paintings by microorganisms arise mainly from the enzymatic decomposition of their constituents, which results in the reduction of the mechanical strength of the support and loss of flexibility of paint layers [7, 8, 15-18]. Actinomycetes are known to produce many types of enzyme such as collagenases (proteases), which are capable of destroying collagen and gelatin-based binders by their hydrolytic activity. Collagenases cleave the collagen molecule into short peptides by hydrolysis at multiple sites along the triple helix. These enzymes are capable of recognizing small amino acid sequences in the protein chain and, therefore, act on active sites along the collagen molecule, which are dictated by the primary structure (amino acid sequence) rather than by the entire molecule configuration. β-collagenase, for instance, cleaves between the X- and the glycine residues in specific sequences: a)-glycine-A-B-glycine-C-alanine-, b) -glycine-B-A-glycine-alanine-arginine-, c) -glycine-B-A-glycine-proline-hydroxyproline- where A-, B- and C- are any of the amino acids present in collagen except glycine. After this, proteases cleave the short peptides released by collagenase action to single amino acids [19].

The main enzymatic activities involved in the deterioration of oil paintings are due to lipases excreted by must fungi. These enzymes catalyze hydrolysis of ester bonds of triacylglycerols at the interface between an insoluble substrate and water [20]. Different biochemical pathways for degradation of lipids by microorganisms have been proposed [1]: a) photooxidation or enzymatic oxidation of the hydrolyzed long chain fatty acids to form free fatty acid hydroperoxydes and then other pertinent end-products [21,22]; b)

the formation of methyl ketones and secondary alcohols from free medium chain fatty acids resulting from metabolism by moulds [21]; c) photooxidation or enzymatic oxidation of triacylglycerols to form triacylglycerol hydroperoxides and further hydrolysis to pass to free fatty acid hydroperoxydes resulting in secondary and tertiary products [21].

As previously mentioned, microorganisms are also responsible for the deterioration of pigments. The fading of the pigments from the Prehistoric cave of Lascaux is the most outstanding example [23]. Di-valent lead-containing pigments such as lead white can be transformed in four-valent lead-oxides by bacteria [24].

In this context, the study of the biodeterioration of reconstructed paint films that mimic historical painting techniques can be of interest for gain knowledge on the mechanisms of biodeterioration, the characterization of the aesthetic changes induced in the painting due to the microorganisms colonization and for establishing its effect in the long-term preservation of the painting due to the loss of chemical and mechanical stability [25]. Classical methodologies for studying paint films biodeterioration are based on electron microscopy [26], chromatographic [22] and spectrophotometric [27-29] techniques. Here, we report for the first time the use of a complementary technique, the voltammetry of microparticles (VMP), for such studies. VMP is a solid-state electrochemical technique developed by Scholz et al. [30,31] which provides analytical information of sparingly soluble insulating solids attached to inert electrodes immersed into suitable electrolytes. Among a variety of materials [32], this technique has been extensively applied in the field of conservation and restoration, as recently reviewed [33,34]. Electrochemistry has also been applied for studying carbon particle distribution in paint films [35], characterization of thin-film porosity [36], electron transfer reactions of membrane-bound proteins and metalloprotein complexes [37].

In the current report, VMP has been used to monitor the deterioration of a series of reconstructed paint films containing cadmium yellow (CdS) bound with two traditional binding media, namely, egg tempera and egg-linseed oil emulsion, which were inoculated with selected fungi and bacteria whose ability for growing in paintings is well known [3,7,8].

Proteinaceous materials and drying oils, either alone or mixed together, have been used since antiquity [38,39]. Egg tempera has been used in paintings, altarpieces and polychromed sculptures in the Middle Ages and, probably, in more ancient times [40]. The whole egg, the yolk or the white can be used as tempera medium. The egg tempera which is traditional and reflects the practice of many centuries is that made simply with yolk of egg. Depending on the degree of opacity to be obtained in the paint layer, the proportions of pigment and medium are adjusted and, if necessary, the whole thinned with water. In general, amounts of pigment around 50% w/w are used [39]. Moreover, in an attempt to obtain particular chromatic, effects artists often used *tempera grassa*, which consists of an emulsion formed by mixing drying oil and egg (whole or yolk) [38].

Cadmium yellow (CdS) is a modern pigment that displays a widely studied electrochemistry in solid state [31-33]. Cadmium yellow was selected as a pigment probe in this study due to its good electrochemical response and its low absorption and scattering in the IR region that enables a complementary study of the changes undergone by the organic binding medium by attenuated total reflectance–Fourier transform infrared spectroscopy (ATR-FTIR). The results obtained from VMP analysis have been complemented with those obtained upon coupling with atomic force microscopy (AFM-VMP) and scanning electrochemical microscopy (SECM). Electrochemical data have also been correlated with field emission scanning electron microscopy (FESEM).

2. Experimental

2.1. Instrumentation

0.25 M sodium acetate buffer (Panreac) at pH 4.75 was used as a supporting electrolyte. Square wave voltammograms (SWVs), and cyclic voltammograms (CVs) were obtained using abrasive VIMP protocols (*vide infra*). Importantly, the electrolyte solution was renewed after each electrochemical run to avoid contamination due to cadmium ions eventually released to the solution phase during electrochemical turnovers. Commercial paraffin-impregnated graphite bars of (Staedtler 200 HB type, 68% wt graphite, diameter 2 mm) were used. Prior to the series of runs for each material or sample, a conditioning protocol was used to increase repeatability. The electrode surface was

polished with alumina, rinsed with water and polished by pressing over paper. For electrode modification, an amount of 1-2 mg of the sample was extended on an agate mortar forming a spot of finely distributed material. Then the lower end of the graphite electrode was gently rubbed over that spot of sample and finally rinsed with water to remove ill-adhered particles. Sample-modified graphite bars were then dipped into the electrochemical cell so that only the lower end of the electrode was in contact with the electrolyte solution. This procedure provides an almost constant electrode area and reproducible background currents.

Electrochemical experiments were performed at 298 K in a three-electrode cell under argon atmosphere using a CH I660C device (Cambria Scientific, Llwynhendy, Llanelli UK). A platinum wire counterelectrode and an Ag/AgCl (3 M NaCl) reference electrode completed the three-electrode arrangement. SECM experiments were performed on deposits of the studied materials on a graphite plate acting as a substrate electrode in contact with 5.0 mM $K_4Fe(CN)_6$ solution in 0.25 M HAc/NaAc (pH 4.75). Experiments were performed with CH 920c equipment using a microdisk platinum electrode tip (CH 49, diameter 20 μm) and a Pt substrate electrode. The bipotentiostat mode was used to apply potentials to the tip (E_T) and the electrode substrate (E_S). In situ AFM-monitored electrochemical experiments were performed with a multimode AFM (Digital Instruments VEECO Methodology Group, USA) with a NanoScope IIIa controller and equipped with a J-type scanner (max. scan size of 150×150×6 μm). The topography of the samples was studied in contact mode. An oxide-sharpened silicon nitride probe Olympus (VEECO Methodology Group, model NP-S) has been used with a V-shaped cantilever configuration. Transference of sample particles to a carbon plate and experimental conditions were similar to those previously described [41,42].

The IR spectra in the ATR mode of the powdered samples were obtained using a Vertex 70 Fourier-transform infrared spectrometer with an FR-DTGS (fast recovery deuterated triglycine sulphate) temperature-stabilised coated detector and a MKII Golden Gate Attenuated Total Reflectance (ATR) accessory. A total of 32 scans were collected at a resolution of 4 cm^{-1} and the spectra were processed using the OPUS/IR software. For performing the determination of the secondary structure of the egg yolk proteins, main features of the commonly used procedure including Fourier Self-Deconvolution (FSD) has been applied. Fourier self-deconvolution (FSD) of the IR spectra covering amide I

region (1595-1705 cm^{-1}) was performed using Lorentzian line shape. Apodization with a Blackman-Harris function was always performed automatically at the same time in the software. FSD was performed using a bandwidth at half height of 13 cm^{-1} and a resolution enhancement factor of 2.4. These values, commonly used for quantitatively estimate the protein secondary structures [43], were selected in an attempt to avoid possible random noise artifacts indistinguishable from amide bands.

Secondary electron images were obtained using a Zeiss field emission scanning electron microscopy (FESEM), model ULTRA 55, operating with a Oxford-X Max X-ray microanalysis system controlled by Inca software. The analytical conditions were: 1 kV accelerating voltage. Samples were directly observed in order to avoid interference with the particulate structure of the coating element used for eliminating charging effects.

2.2. Reference materials and test specimens

Cold pressed linseed oil, and cadmium yellow (CdS) (Kremer) and fresh hen's egg were used as reference materials for preparing the series of paint films. Reconstructed egg tempera paint films (EG) were prepared by mixing the pigment with the appropriate amount of egg until suitable consistence (30% weight composition of pigment); and spreading this product on glass slides in order to form a thin film. The paint films were dried at room temperature during 4 weeks (21ºC, 50% RH). Thickness of the films was in the range 0.3-0.5 mm. Reconstructed egg + linseed oil emulsion paint films (EO) were prepared by mixing the pigment with the appropriate amount of an egg-linseed oil emulsion (1:1) (35% weight composition of pigment). The reconstructed paint films were dried at room temperature during 4 weeks (21ºC, 50% RH). Thickness of the films was in the range 0.3-0.5 mm.

2.3. Microorganisms and cultures

Bacterial and fungal strains, obtained from the Spanish Collection of Type Cultures (CECT, Colección Española de Cultivos Tipo, Universidad de Valencia, Valencia, Spain), were chosen because they have been frequently found in biodeterioration studies of cultural heritage [8]. The selected fungi were: *Acremonium crhysogenum* (Ac) (CECT 2718, ATCC 14615), *Aspergillus niger* (An) (CECT 2088, ATCC 9029), *Mucor*

roxii (Mr) (CECT 2655, ATCC 24905), *Penicillium chrysogenum* (Pc) (CECT 2306, ATCC 8537) and *Trichoderma pseudokoningii* (Tp) (CECT 2937). The selected bacteria were: *Arthrobacter oxydans* (Ao) (CECT 386, ATCC 14358), *Bacillus amyloliquefaciens* (Ba) (CECT 493, ATCC 23842) and *Streptomyces celluloflavus* (Sc) (CECT 3242, ATCC 29806).

Bacteria were grown on culture plates of Trypticase Soy Agar (TSA, Scharlau) medium and were incubated at 28ºC for 24 hours. To obtain bacterial suspensions, cells from liquid cultures were centrifuged and washed to remove possible remains of the culture medium. Bacterial suspensions were adjusted to 10^7cells mL^{-1}. To obtain fungal spores, fungi were grown on Potato Dextrose Agar (PDA, Scharlau, Barcelona, Spain) over a total period of one week at 28ºC and spores were collected by washing the culture with distilled water with 0,1% Tween 80 (Aldrich) and filtering through sterile glass wool. The resulting suspensions of spores were centrifuged three times and the supernatants were discarded in order to avoid any residue from the culture medium or rest of mycelia. Finally, spores were re-suspended in 1 mL ultrapure water and spores suspensions were adjusted to 10^5-10^6 spores mL^{-1}.

2.4. Inoculation and incubation of paint specimens

Reconstructed paint films prepared as egg yolk tempera (EG) and egg-oil emulsion (EO) were inoculated with three separated drops of 20 µL of each fungal and bacterial suspension. After inoculation, each paint film was placed in the center of a Petri dish and incubated in darkness for 40 days at 28ºC, 80% relative humidity. Thus, two series of biodeteriorated reconstructed paint films were obtained (EG@microorganism and EO@microorganism). Paint films inoculated with 20 µL of sterile ultrapure water and incubated under the same conditions were used as controls (EG@Blank and EO@Blank). After incubation, the microbial biomass was completely removed from the surface of the reconstructed paint films.

3. Results and discussion

3.1. Film micromorphology

It is well known that microscopically, egg yolk has a variety of multi-scale structures that are suspended in a yellowish and continuous fluid phase (plasma) [44]. This complex structure determines the formation of a paint layer from drying of egg yolk medium and egg-oil emulsions, which has been described as a process that involves two steps. A first step of evaporation of the water from the plasma takes place until reaching equilibrium with the humidity of the surrounding air. The loss of water results in the appearance of intermolecular empty spaces and loss of hydrogen bonding that force the molecules of protein to rearrange their chains to maximize their intra and interchain hydrogen bonding to replace lost hydrogen bonds to water. Prior spectroscopic studies have demonstrated that structural changes undergone by proteins on dehydration are predominantly related to conformational transitions that results in a final dried state in which the preferred conformation adopted by the protein is β-sheet regardless of the initial conformation in aqueous solution. This is due to the lower degree of solvation required by this conformation [45].Thus, the protein molecules adopt more unordered conformations in which most side chain groups become now available with the consequent increase of the chemical activity of the protein molecule with other molecules (protein, triglycerides, metal ions solubilised from pigment grains, …) [45,46]. Finishing of the drying process has been proposed via a further step of formation of a protein network accompanied of coalescence and reticulation of glycerolipids [39, 47] that results in a continuous medium that binds the pigment grains as it can be seen in Figure 1a, which shows the FESEM secondary electron image of the cross-section of an un-inoculated egg tempera paint film. In this reconstructed paint film, the pigment grains, with size below 1 μm, are bound by a binder that mainly consists of dried egg yolk plasma. A number of spheres and granules, typical multi-scale structures of egg yolk that are insoluble denser protein-lipid particles (∅:4-150 μm and ∅:0.2-2 μm, respectively), can also be identified.

Figure 1b shows the FESEM secondary electron image of the cross-section of an un-inoculated reconstructed egg-oil emulsion paint film. As it can be seen, the pigment grains are completely embedded by the binding medium that, in this case, is a mixture of polymerized linseed oil and egg yolk plasma. Presence of linseed oil results in a most complete embedding of pigment grains. Spheres and granules are here hardly identified (see arrows) due to the presence of linseed oil.

Inoculation of paint films consisted of applying a drop of water containing the different microorganisms in study followed by incubation in a chamber maintained at a high level of humidity. Contact of the dried paint film with the aqueous phase can induce changes in the structure of the film. First of all, hydrolysis of triglycerides can be promoted resulting in releasing of notable amounts of fatty acids. Hydrolysis of proteins can also take place resulting in the cleavage of the protein molecules, whose shorter fragments can also migrate to the aqueous phase. As the evaporation of the drop is carried out in a brief period, the final result is the appearance of micropores and the migration of the solubilized species from the film core to the surface where are concentrated and/or vaporized at more or less extent. After this, bacteria and fungi start their attack settling the external surface and pores, as can be seen in Figure 2.

3.2. VMP, SECM and AFM-VMP analysis

Figure 3a shows the cyclic voltammogram of a microparticulate deposit of cadmium yellow pigment on graphite electrode immersed into acetate buffer at pH 4.75. A reduction wave at ca. −1.0 V vs. Ag/AgCl (C_1) accompanied by a shoulder at ca. −1.2 V (C_2) which precedes the rising current for solvent discharge is recorded in the initial cathodic scan. In the subsequent anodic scan, a main oxidation signal at −1.1 V (A_1) appear. Following literature [37-40], the peak C_1 can be attributed to the reduction of CdS to Cd metal which is subsequently oxidized, upon reversal the potential scan, to Cd^{2+} (aq) in the stripping process A_1. This process has been widely studied for cadmium determination in aqueous solution [48,49]. The C_2 signal can be tentatively assigned to the reduction of H^+ and/or Cd^{2+} ions released during the reduction of CdS on the Cd-plated graphite surface.

This voltammetry becomes significantly modified for samples excised from the reconstructed paint films. As can be seen in Figs. 3b,c, the C_2 shoulder disappears whereas the shape of the peaks C_1 and A_1 varies. In the case of EG@Blank paint film (Fig. 3b), a new cathodic process is recognized by the signal at −0.70 V (C_3) preceding the peak C_1 at −0.95 V, the voltammetric profile remaining essentially unchanged in the second and successive potential scans. For EO@Blank specimens (Fig. 3c), the initial cathodic scan displays an additional signal at −0.80 V (C_4) is overlapped to peaks C_1

and C_3 (weak), but in the second and successive scans, only peaks C_1 and C_4 remain. In all cases, upon increasing potential scan rate between 0.01 and 0.50 V s^{-1}, the peaks C_3 and C_4 become enhanced relative to the peak C_1, but the voltammetric profile becomes ill-defined. The anodic region of the voltammograms is similar in all cases, with stripping peak A_1 at –0.75 V preceding a wider oxidation peak (A_3) at ca. –0.50 V when the peak C_3 appears. Interestingly (*vide infra*), when the peak C_4 appears, the stripping of Cd consist of a unique peak A_1.

SECM examination of EG and EO reconstructed paint films attached to a graphite plate in contact with $K_4Fe(CN)_6$ solution in acetate buffer is illustrated in Figure 4. Application to the tip of a potential high enough (E_T = +0.30 V) to promote the diffusion-controlled oxidation of $Fe(CN)_6^{4-}$ ions, yields a current response depending on the topography and conductivity of the substrate. The map colors yield positive feedback features corresponding to the pigment grains emerging from the binding medium which appears as an almost uniform negative feedback background. Apart from textural differences between EG@CdS and EO@CdS films (Figs. 4a,c, respectively), in both cases, after application of a potential input of –1.0 V during 5 min, there appears significant changes in the map color (Figs. 4b,d, respectively), thus denoting that the reduction of CdS operates under these conditions. As a result of the application of this reductive potential input, the area of positive feedback features become diminished just such as embedded by a growing binding media.

Figure 5 depicts the AFM images recorded before (Figs. 5 a,b) and after (Figs. 5 c,d) application of a potential input of –1.0 V to a egg tempera reconstructed paint film (EG@Blank) during 5 min. Apparently, the pigment grain, which is partially in contact with the base graphite plate, experiences a contraction process being reduced, at the end of the reductive step, to a grain whose volume is ca. one half of the volume of the original pigment grain. This result would be in agreement with data reported by Hasse and Scholz on *in situ* XRD [50] and AFM [51] monitoring of the reduction of litharge, where the reduction of the mineral crystals involves a topotactic solid state transformation of lead oxide to lead metal without a morphological disintegration. This model would apply here, the volume contraction expected in the reduction of CdS to Cd being consistent with the different density of CdS (4.83 g cm^{-3}) and Cd (8.65 g cm^{-3}). Interestingly, the topography

of the binder surrounding the grain is smoothed in the vicinity of the same.

All these results can be rationalized on considering that the EG and EO reconstructed paint films are constituted by a more or less homogeneous distribution of pigment particles more or less entirely embedded by a layer of more hydrophobic binding medium and a hydrophilic layer where resulting secondary cadmium compounds exist, as described for pictorial specimens containing lead pigments [41]. Under VMP conditions, the voltammetric signals correspond to the particles in contact with the base graphite electrode and the electrolyte [31-33]. Accordingly, the CdS-centered reduction processes can be described in terms of:

a) Peak C_1 corresponds to the reduction of CdS grains exposed to the graphite surface:

$$\{CdS\}_{solid} + 2H^+_{aq} + 2e^- \rightarrow \{Cd\}_{solid} + H_2S \quad (1)$$

The subsequent oxidation of the Cd deposit to Cd^{2+} ions in solution gives rise to the stripping peak A_1.

b) Peak C_3 appearing in EG reconstructed paint films can be attributed to the reduction of the Cd compounds forming the ionomeric layer accompanying the pigment particles. This layer, to some extent similar to that formed in the reduction of lead minerals [48,51], would be particularly relevant for the proteinaceous fraction of the binders (egg) disposing of coordinating units. The reduction process can be represented as:

$$\{Cd^{2+}(binding^{2-})\}_{CdS\ ionomeric\ layer} + 2H^+_{aq} + 2e^- \rightarrow \{Cd\}_{solid} + H_2binding \quad (2)$$

This process results in a deposit of Cd metal different to that resulting from the reduction C_1. The subsequent oxidation process A_3 appears at potentials clearly differing from those of peak A_1, a feature consistent with the electrochemistry of different minerals [41,42].

c) Peak C_4, typical of EO reconstructed paint film, would be representative of the reduction of CdS particles surrounded by binding media dominated by the linseed oil fraction of such specimens. Then, Cd soaps would appear where Cd(II)-carboxylate

complexes were formed. The corresponding reduction process can be represented as:

$$\{Cd^{2+}(RCOO^{-})_2\}_{Cd\ soap} + 2H^{+}_{\ aq} + 2e^{-} \rightarrow \{Cd\}_{solid} + 2RCOOH \qquad (3)$$

The deposit of Cd metal formed here would be similar to that formed by electrochemical reduction of bare CdS particles, so that it is oxidized at an identical or almost identical potential (peak A_1).

3.2. VMP testing of biodeterioration

The voltammetric response of the reconstructed paint films is differently modified after inoculation. Figure 6 shows cyclic voltammograms for the egg-oil emulsion paint films after inoculation with two fungi, *Aspergillus Níger* (EO@An) (Fig. 6a) and *Acremonium crhysogenum* (EO@Ac) (Fig. 6b), and two bacteria, *Bacillus amyloliquefaciens* (EO@Ba) (Fig. 6c) and *Arthrobacter oxydans* (EO@Ao) (Fig. 6d), respectively. One can observe that the fungi attack leads to voltammograms displaying only the peak C_1, eventually accompanied of weak signal C_4. In contrast, after bacteria attack, the voltammograms consist of 'clean' peaks C_3 and C_1 with no traces of peak C_4.

The voltammetry of the reconstructed egg tempera paint films (EG) inoculated with both fungi and bacteria (see Fig. 7) was relatively close to that of bare cadmium yellow in Fig. 3a, with well-defined peak C_2. The most significant differences were the appearance of additional cathodic peaks at potentials more negative than C_1, labeled as C_5 and marked by arrows in Fig. 7, and the appearance of peak splitting in peak A_1, now accompanied by peak A_3. The peak C_5 can be attributed to the reduction of CdS surface complexes associated to the proteinaceous fraction which was modified by the biological attack (*vide infra*). This process can, in principle, be represented also by Eq. (2).

Consistently with the scheme in section 3.1, in EO paint films, bacteria attack would be concentrated on the most abundant oil fraction of the binding medium so that the reduction of pigment particles (C_1) and their ionomeric layer (C_3) remain well-defined, while the signal C_4 disappears. On the contrary, fungi attack, although affecting both ionomeric and oil fractions, appears to be concentrated in the proteinaceous fraction, so

that peak C_3 entirely disappears while the signal C_4 becomes significantly decreased.

Additional information can be obtained from electrochemical data in the region of positive potentials. Figure 8 compares linear scan voltammograms for a) pure pigment CdS, b) pure egg yolk and reconstructed egg tempera paint films c) before EG@blank and d) after inoculation with *Aspergillus niger* (EG@An). The pigment displays a well defined anodic peak at +0.82 V (A_{CdS}) preceded by a shoulder at ca. +0.65 V. Although sulfur electrochemistry is complicated [53], the oxidation of CdS can be represented as [31-33]:

$$\{CdS\}_{solid} \rightarrow \{S\}_{solid} + Cd^{2+}{}_{aq} + 2e^{-} \quad (4)$$

In turn, reconstructed egg tempera paint films produce an oxidation signal consisting of overlapping voltammetric peaks centered at +0.45 V (A_{PR}), attributable either to the oxidation of metalloprotreins [54] and/or –SH units of proteins [55]. The un –inoculated egg tempera paint film (EG@blank) yields a voltammetric response dominated by the signal A_{PR}, whose profile is slightly modified, while the A_{CdS} signal becomes considerably lowered. Consistently with the foregoing set of voltammetric data, the effect of fungi and bacteria on the voltammetry of EG paint film was similar, now significantly lowering both A_{CdS} and A_{PR} features.

In contrast, the voltammetry of inoculated reconstructed egg-oil emulsion paint films shows differences between fungi and bacteria. These can be seen in Figure 9, where linear scan voltammograms for films of: a) pure egg + linseed oil emulsion; b) EO@Blank and reconstructed EO paint film inoculated with c) *Bacillus amyloliquefaciens* (EO@Ba) and d) *Aspergillus niger* (EO@An), are depicted. The binder film (Fig. 9a) produces an oxidation signal at –0.08 V (A_{LO}), which could be tentatively attributed to the oxidation of tocopherols. These are components of linseed oil [56,57] displaying a well-defined oxidative electrochemistry [58,59]. In the presence of CdS (Fig. 9b), this signal is accompanied by minor signals at +0.45 (A_{B1}) and +0.60 (A_{B2}) preceding the CdS-centered oxidation (A_{CdS}) at +0.82 V. These signals can be attributed to electrochemically oxidizable compounds resulting from the interaction between CdS and the binder. This would be consistent with results from Madani et al. [60] on the effect of CdS on polymerization reactions. Interestingly, after bacterial

attack (Fig. 9c), the A_{CdS} and A_{B1} peaks disappear whereas the peak A_{B2} is enhanced. In contrast, fungi attack (Fig. 9d) results in the maintenance of peaks A_{CdS} and A_{B2} peaks with lowering/disappearance of peak A_{B1}. These results indicate that the presence of the pigment produce reaction chains in the binder resulting in products which react selectively with fungi and/or bacteria in the paint film.

3.3. FTIR spectroscopy

In order to validate VMP analysis of biodeterioration, ATR-FTIR spectroscopy was applied. This technique enables the recognition of changes in the chemical composition and structure of both triglycerides and proteins conforming traditional binding media used in art so that it has been a useful complementary analytical technique in order to identify changes in the composition of the paint specimens [27,61,62]. Un-inoculated egg tempera specimen (EG@Blank in Figure 10) exhibited an IR spectrum dominated by the amide A (3300 cm^{-1}), amide I (1635 cm^{-1}) and amide II (1537 cm^{-1}) bands and the -CH_3 and -CH_2- stretching vibrations (2924 and 2858 cm^{-1}) [27,61,62]. Band associated to the ester groups in triglycerides C=O stretching vibrations at 1742 cm^{-1} and shoulder at 1736 cm^{-1} attributed to phospholipids, accompanied of the C-O stretching pattern at 1234, 1163 and 1086 cm^{-1} were also identified. The latter bands are prevalent in un-inoculated egg plus linseed oil emulsion paint film (EO@Blank in Fig. 10). Hydrolysis of triglycerides was confirmed in both specimens EG@Blank and EO@Blank by the appearance of several shoulders in the range (1736-1710 cm^{-1}) ascribed to free fatty acids released as result of processes of hydrolysis of oil and egg triglycerides [27,28,62].

Application of FTIR spectroscopy to the analysis of protein secondary structure is based on the sensitivity of peptide group IR absorptions to the protein chain conformations. These structural modifications can be observed in the amide I region, which exhibits the highest protein conformational sensitivity [63]. By contrast to the aqueous solutions, protein solid films exhibit a higher crystalline structure [64]. Our findings in this region, described below, are presented in terms of the position of the amide I sub-bands. Position of the sub-bands was determined from the deconvolved IR spectra (Figure 11) [43]. Amide I bands of EG@Blank and EO@Blank show typical profile characteristic of β-sheet conformation predominant in dried globular proteins of albuminoid type [65]

with a prominent maximum centered at 1635 cm^{-1} in EG@Blank and 1628 cm^{-1} in EO@Blank that, according to recent literature [43,65,66], is ascribed to intramolecular β-sheet conformations. The redshift observed in the position of the maximum for egg-oil emulsion film could be associated to changes in the β-sheet conformations of protein molecules [66], probably occurring as result of the appearance of intermolecular interactions of the protein molecules with the oil triglycerides and their oxidation and hydrolysis products [47]. The secondary maximum at 1643 cm^{-1} in EG@Blank and at 1648 cm^{-1} in EO@Blank is ascribed to the unordered (random coil) conformation [66]. Both specimens EG@Blank and EO@Blank exhibited secondary maxima at 1652 cm^{-1}, with shoulders at 1658 and 1660 cm^{-1} ascribed to helical conformation [65]. Shoulders at 1625 and 1619 cm^{-1} are ascribed to intermolecular β-sheet structures [67] whereas shoulders at 1668, 1674, 1683, 1688 and 1694 cm^{-1} are ascribed to β-turn conformations [43,63].

Microbial attack in the reconstructed tempera films resulted in all cases in the decrease of the relative content in carbonyl band to amide I and II bands (see Table 1). This decrease is more evident in the series of reconstructed egg-oil emulsion films since this reduction in the carbonyl band has been associated to the loss of lipids as result of the enzymatic oxidation of the hydrolyzed long chain fatty acids to form free fatty acid hydroperoxydes and then other volatile end-products. This hypothesis is confirmed by the increase in the content of free fatty acids formed as consequence of the hydrolysis of the triglycerides and phospholipids observed from the enhancement of bands around 1725-1700 cm^{-1}. Hydrolysis of triglycerides and further loss of end-products of ketone and aldehyde type is taking place at lesser extent in egg yolk due to its particular microstructure with a variety of insoluble particles (see Fig. 1a) with structure of micellar complexes in which triglycerides and cholesterol forms the core of the particle that is surrounded by an amphipathic surface monolayer of phospholipids, proteins and unesterified cholesterol [68-71] that prevent the oxidation of triglycerides inside.

Comparison of band area ratio obtained in the specimens inoculated with the selected fungi and bacteria shows that, in general, bacteria are more efficient in promoting loss of lipids than fungi apart from the fungus *Mucor roxii* that showed a particular ability for promoting deterioration of both types of paint films. These results are in good

agreement with those previously reported from oil-varnish specimens inoculated with several species of microorganisms, where a remarkable increase of the hydrolysis reactions was detected [72].

Changes in the proteinaceous materials present in the series of inoculated egg tempera paint films can be seen in Figure 11a that shows the amide I bands of the blank (EG@Blank) and inoculated reconstructed egg yolk tempera paint films. Modification of the profile of this band inform of an alteration in the secondary structure of the proteins, which could be relied with the microbial degradative activity. Fungi exhibit more remarkable changes with red-shift of the maximum in the intramolecular β-sheet region from 1635 cm^{-1} to 1633 cm^{-1} for EG@Ac and EG@An and 1631 cm^{-1} for EG@Mr and EG@Tp. Band at 1625 cm^{-1} ascribed to intermolecular β-sheet conformations is also enhanced in specimens inoculated with fungi. These conformations are typical of aggregated proteins [65]. Enhancement of band ascribed to random coil conformations in the range 1645-1648 cm^{-1} is also observed in the paint films inoculated with fungi. This last result suggests that attack of these microorganisms result in an increase in the irregular structures and, in particular, in a partial opening of the ordered structure into random turns and bends. This would be consistent with the disappearance of the peak C_3 and the appearance of peak C_5 in the corresponding voltammograms (see Fig. 7).

In the case of egg-linseed oil emulsion paint films (see Figure 11b), the more remarkable changes observed in the shape of the amide I band of inoculated specimens were also found in reconstructed paint films inoculated with fungi. Blue-shift of the maximum in the intramolecular β-sheet region from 1628 cm^{-1} to 1631 cm^{-1} for EO@Tp, 1634 cm^{-1} for EO@An, EO@Mr and EO@Pc and 1636 cm^{-1} for EO@Ac are observed. In all these specimens, new bands associated with random coil conformations were recognized at 1640 cm^{-1} for EO@An, EO@Mr and EO@Tp, at 1645 cm^{-1} for EO@An, EO@Mr and EO@Pc and at 1647 cm^{-1} for EO@Ac. Finally, a notable increase in the content of free fatty acids is also observed in these specimens (relative growth of bands in the range 1725-1700 cm^{-1}). Presence of fatty acids could contribute to promote new unordered conformations in the egg proteins characterized by being more loosened and unfolded due to the net positive charge in a more acidic solution.

This net positive charge results in a more random structure due to the repulsion between turns and bends that increase the positive net charge [65].

All these features would be consistent with the ascription of the voltammetric process C_3 in EG@Blank specimens to the coordination of CdS to proteins mainly disposed in β-sheet conformation. Under attack of both bacteria and fungi (see Fig. 7), random coil conformations are increased, here appearing the peak C_5 to the coordination of proteins in aggregated and more disordered structures to the pigment surface while the C_3 signal disappears. In the case of the EO@CdS specimen, peak C_4 would be associated to the reduction of Cd soaps formed as the result of complexation of Cd with the carboxylate groups of fatty acids of the linseed oil fraction. In such specimen, the attack of bacteria and fungi results in the formation of complexes with proteins, probably favored by the opening and unfolding of their secondary structure thus producing the re-appearance of peak C_3 (see Fig. 6), this effect being more intense for bacteria than for fungi. Table 2 summarizes the description of electrochemical processes associated to biodeterioration of un-inoculated and inoculated reconstructed EG and EO paint films.

4. Conclusions

In contact with aqueous acetate buffer, VMP data denote that in presence of the binder, the voltammetric signals for CdS in reconstructed egg tempera and egg-linseed oil emulsion paint films become modified with appearance of specific signals resulting from the pigment-binder association. Such voltammetric responses varied after attack with different fungi (*Acremonium crhysogenum*, *Aspergillus niger*, *Mucor roxii*, *Penicillium chrysogenum*, and *Trichoderma pseudokoningii*) and bacteria (*Arthrobacter oxydans*, *Bacillus amyloliquefaciens*, and *Streptomyces cellulofans*). Combining VMP data with those from ATR-FTIR, SECM, FESEM and AFM, suggests that specific cathodic signals can be attributed to the reduction of Cd ions bound to proteins that have acquired a more open and unfolded conformation, and the reduction of Cd soaps formed as the result of complexation with the carboxylate groups of fatty acids of the linseed oil fraction. Depending on the binder and the biological agent, such signals become more or less modified after biodeterioration, then allowing for discriminating bacterial and fungi attacks. This multi-technique study also indicates that microbial attack results in

the increase of the content of free fatty acids released from the catalyzed hydrolysis of triglycerides from oil and egg as well as in the breaking down of proteins accompanied of an increase in the irregular and open conformations adopted by the protein molecules. These results are in good agreement with the observed changes in the mechanical behavior of the inoculated specimens.

Aknowledgements.- This work as been performed by members of the microcluster *Grupo de análisis científico de bienes culturales y patrimoniales y estudios de ciencia de la conservación* (Ref. 1362) belonging to the Valencia International Campus of Excellence. Financial support is gratefully acknowledged from the Spanish "I+D+I MICINN" projects CTQ2014-53736-C3-1-P and CTQ2014-53736-C3-2-P supported by ERDF funds. The authors whish to thank Dr. José Luis Moya López and Mr. Manuel Planes Insausti (Microscopy Service of the Universitat Politècnica de València) for technical support.

References

[1] Ratledge C (1994) Biochemistry of microbial degradation. Springer, Berlin

[2] Caneva G, Nugari MP, Salvadori O (2008) Plant Biology for Cultural Heritage, The Getty Conservation Institute, Los Angeles

[3] Sterflinger K (2010) Fungi: Their role in deterioration of cultural heritage. Fungal Biology Reviews 47 – 55 and references therein. doi: 10.1016/j.fbr.2010.03.003

[4] Gargani G (1968) Fungus contamination of Florence art masterpieces before and after the 1966 disaster. In: Walters AH, Elphick JJ (eds.) Biodeterioration of Materials, Elsevier, Amsterdam, pp 252-257

[5] Seves AM, Sora S, Ciferr O (1996) The microbial colonization of oil paintings – A laboratory investigation. Int Biodeter Biodegr 37:215-224.
doi: 10.1016/S0964-8305(96)00006-6

[6] Tiano P (2002) Biodegradation of cultural heritage: Decay mechanisms and control methods. Online at http://www.arcchip.cz/w09/ w09_tiano.pdf.

[7] Strzelczyk AB (2004) Observations on aesthetic and structural changes induced in Polish historic objects by microorganisms. Int Biodeter Biodegr 53:151–156. doi: 10.1016/s0964-8305(03)00088-x

[8] López-Miras M, Piñar G, Romero-Noguera J, Bolivar-Galiano FC, Ettenauer J, Sterflinger K, Martín-Sánchez I (2013) Microbial communities adhering to the obverse and reverse sides of an oil painting on canvas: identification and evaluation of their biodegradative potential. Aerobiologia 29:301–314. doi: 10.1007/s10453-012-9281-z

[9] Koszewski A, Rymuza Z, Reuther F (2008) Evaluation of nanomechanical, nanotribological and adhesive properties of ultrathin polymer resist film by AFM. Micro Engn 85:1189–1192. doi: 10.1016/j.mee.2008.01.025

[10] Schabereiter-Gurtner C, Piñar G, Lubitz W, Rölleke S (2001) An advanced molecular strategy to identify bacterial communities on art objects. J Microbiol Meth 45:77–87. doi: 10.1016/s0167-7012(01)00227-5

[11] Florian MLE (1996) The role of the conidia of fungi in fox spots. Stud Conserv 41:65-75. doi: 10.2307/1506518

[12] Arai H, Matsui N, Matsumura N, Murakita H (1988) Biochemical investigations on the formation mechanisms of foxing. Stud Conserv 33:11-12. doi: 10.1179/sic.1988.33.1.11

[13] Arai H, Matsumura N, Murakita H (1990) Microbiological studies on the conservation of paper and related cultural properties: Part 9, induction of artificial foxing. Science for Conservation 29:25-34.

[14] Hayashi T, Namili M (1986) Role of sugar fragmentation in early stage browning

of amino-carbonyl reaction of sugars with amino acids. Agr Biol Chem Tokyo 50:1965-1970. doi: 10.1080/00021369.1986.10867692

[15] Allsopp D, Seal KJ, Gaylarde ChC (2004) Introduction to biodeterioration, 2nd Ed, Cambridge University Press, Cambridge

[16] Bock E, Sand W (1993) The microbiology of masonry biodeterioration. J Appl Bacteriol 74:503-514. doi: 10.1111/j.1365-2672.1968.tb00384.x

[17] Ciferri O (2002) The role of microorganisms in the degradation of cultural heritage. Reviews in Conservation. 3:35-45. doi: 10.1179/sic.2002.47.Supplement-1.35

[18] Van der Snickt G, Dik J, Cotte M, Janssens K, Jaroszewicz J, De Wolf W, Groenewegen J, Van der Loeff L (2009) Characterization of a degraded cadmium yellow (CdS) pigment in an oil painting by means of synchrotron radiation based X-ray techniques. Anal Chem 81:2600-2610. doi: 10.1021/ac802518z

[19] Child AM (1995) Microbial taphonomy of archaeological bone. Stud Conserv 40:19-30. doi: 10.1179/sic.1995.40.1.19

[20] Soliman NA, Knoll M, Abdel-Fattah YR, Schmid RD, Lange S (2007) Molecular cloning and characterization of thermostable esterase and lipase from Geobacillus thermoleovorans YN isolated from desert soil in Egypt. Process Biochem 42 (2007)1090–1100. doi: 10.1016/j.procbio.2007.05.005

[21] Kinderlerer JL (1994) Degradation of the lauric acid oils. Int Biodeter Biodegr 33 (1994) 345–354. doi: 10.1016/0964-8305(94)90012-4

[22] Berg JDJ van den, KJ van den, Boon JJ (2002) Identification of non-cross-linked compounds in methanolic extracts of cured and aged linseed oil-based paint films using gas chromatography-mass spectrometry. J Chromatogr A 950:195–211 (and references therein). doi: 10.1016/s0021-9673(02)00049-3

[23] Lefèvre M (1974) La ‘maladie verte’ de Lascaux. Stud Conserv 19:126-156. doi: 10.2307/1505660

[24] Petushkova JP, Lyalikova NN (1986) Microbiological degradation of Lead-containing pigments in mural paintings. Stud Conserv 31:65-69. doi: 10.2307/1506003

[25] Breitbach AM, Rocha JC, Gaylarde CC (2011) Influence of pigment on biodeterioration of acrylic paint films in Southern Brazil. J Coat Technol Res 8:619–628.
doi: 10.1007/s11998-011-9350-1

[26] Keune K, van Loon A, Boon JJ (2011) SEM Backscattered-Electron Images of Paint Cross Sections as Information Source for the Presence of the Lead White Pigment and Lead-Related Degradation and Migration Phenomena in Oil Paintings. Microsc Microanal 17:696-701. doi:10.1017/S1431927610094444

[27] Meilunas RJ, Bentsen JG, Steinberg A (1990) Analysis of aged paint binders by

FTIR Spectroscopy. Stud Conserv 35:33-51. doi:10.2307/1506280

[28] Mazzeo R, Prati S, Quaranta M, Joseph E, Kendix E, Galeotti M (2008) Attenuated total reflection micro FTIR characterization of pigment–binder interaction in reconstructed paint films. Anal Bioanal Chem 392:65-76. doi: 10.1007/s00216-008-2126-5

[29] Salvadó N, Butí S, Nicholson J, Emerich H, Labrador A, Pradell T (2009) Identification of reaction compounds in micrometric layers from gothic paintings using combined SR-XRD and SR-FTIR. Talanta 79:419-428. doi: 10.1016/j.talanta.2009.04.005

[30] Scholz F, Meyer B (1998) Voltammetry of solid microparticles immobilized on electrode surfaces. Electroanal Chem 20:1–86.

[31] Scholz F, Schröder U, Gulabowski R, Doménech-Carbó A (2014) Electrochemistry of Immobilized Particles and Droplets, 2nd edit. Springer, Berlin-Heidelberg

[32] Doménech-Carbó A, Labuda J, Scholz F (2013) Electroanalytical chemistry for the analysis of solids: characterization and classification (IUPAC Technical Report), Pure Appl Chem 85:609–631. doi: 10.1351/PAC-REP-11-11-13

[33] Doménech-Carbó A, Doménech-Carbó MT, Costa V (2009) Electrochemical Methods for Archaeometry, Conservation and Restoration (Monographs in Electrochemistry Series F. Scholz, Edit.). Springer, Berlin-Heidelberg

[34] Doménech-Carbó A (2010) Electrochemistry for Conservation science. J. Solid State Electr 14:349-351. doi: 10.1007/s10008-009-0934-y

[35] Mozetic M, Zalar A, Panjan P, Bele M, Pejovnik S, Gmek R (2000) A method of studying carbon particle distribution in paint films. Thin Solid Films 376:5-8. doi: 10.1016/s0040-6090(00)01347-x

[36] Sittner F, Ensinger W (2007) Electrochemical investigation and characterization of thin-film porosity. Thin Solid Films 515:4559-4564. doi: 10.1016/j.tsf.2006.11.031

[37] Kuznetsov AM, Ulstrup J (1989) Protein dynamics and electronic fluctuation effects in electron transfer reactions of membrane-bound proteins and metalloprotein complexes. J Electroanal Chem 275:289-305. doi: 10.1016/0302-4598(89)85008-1

[38] Matteini M, Moles A (1989) La Chimica nel Restauro. Nardini, Firenze

[39] Gettens RJ, Stout GL (1966) Painting Materials. A Short Encyclopedia. Dover Publications, New York

[40] Cennini C (1982) Il libro dell' arte. Akal, Madrid.

[41] Doménech-Carbó A, Doménech-Carbó MT, Mas-Barberá X (2007) Identification of lead pigments in nanosamples from ancient paintings and polychromed sculptures using voltammetry of nanoparticles/atomic force microscopy. Talanta 71:1569-1579.

doi: 10.1016/j.talanta.2006.07.053

[42] Doménech-Carbó A, Doménech-Carbó MT, Silva M, Valle-Algarra FM, Gimeno-Adelantado JV, Bosch-Reig F, Mateo-Castro R (2015) Screening and mapping pigments in paintings using scanning electrochemical microscopy (SECM). Analyst 140:1060-1075.
doi: 10.1039/c4an01911c

[43] Byler DM, Susi H (1986) Examination of the Secondary Structure of Proteins by Deconvolved FTIR Spectra. Biopolymers 25:469-487. doi: 10.1002/bip.360250307

[44] Chang CM, Powrie WD, Fennema O (1977) Microstructure of egg yolk. J Food Sci 42:1193-1200. doi: 10.1111/j.1365-2621.1977.tb14458.x

[45] Prestrelski SJ, Tedeschi N, Arakawa T, Carpenter JF (1993) Dehydration-induced Conformational Transitions in Proteins and Their Inhibition by Stabilizers. Biophys J 65:661-671. doi: 10.1016/s0006-3495(93)81120-2

[46] Boehm S, Abaturov LV (1977) Structural Changes of Met-haemoglobin by Dehydration. Febs Lett 77: 21-24. doi: 10.1016/0014-5793(77)80184-1

[47] Karpowicz A (1981) Ageing and deterioration of proteinaceous media. Stud Conserv 26:153-160. doi: 10.2307/1505885

[48] Suciu P, Vega M, Roman L (2000) Determination of cadmium by differential pulse adsorptive stripping voltammetry. J Pharmaceut Biomed 23:99-106.
doi: 10.1016/s0731-7085(00)00279-x

[49] Koper A, Grabarczyk M (2012) Simultaneous voltammetric determination of trace bismuth(III) and cadmium(II) in water samples by adsorptive stripping voltammetry in the presence of cupferron, J Electroanal Chem 681:1-5. doi: 10.1016/j.jelechem.2012.05.020

[50] Meyer B, Ziemer B, Scholz F (1995) *In Situ* X-Ray Diffraction Study of the Electrochemical reduction of Tetragonal Lead oxide and Orthorhombic Pb(OH)Cl Mechanically Immobilized on a Graphite Electrode. J Electroanal Chem 392:79-83.

[51] Hasse U, Scholz F (2001) In situ atomic force microscopy of the reduction of lead oxide nanocrystals immobilised on an electrode surface. Electrochem Commun 3:429-434. doi: 10.1016/s1388-2481(01)00194-1

[52] Eissler RL, Princen RH (1972) The interface between reactive pigment and binder matrix. J Electroanal Chem 37:327-336. doi: 10.1016/s0022-0728(72)80237-7

[53] Colletti LP, Teklay D, Stickney JL (1994) Thin-layer electrochemical studies of the oxidative underpotential deposition of sulfur and its application to the electrochemical atomic layer epitaxy deposition of CdS. J Electroanal Chem 369:145-152. doi: 10.1016/0022-0728(94)87092-6

[54] Hu N (2001) Direct electrochemistry of redox proteins or enzymes at various film electrodes and their possible applications in monitoring some pollutants. Pure Appl Chem 73:1979-1991. doi: 10.1351/pac200173121979

[55] Ralph TR, Hitchman ML, Millington JP, Walsh FC (1994) The electrochemistry of L-cystine and L-cysteine: Part 1: Thermodynamic and kinetic studies. J Electroanal Chem 375:1-15. doi: 10.1016/0022-0728(94)03407-9

[56] Sutherland K (2003) Solvent-Extractable Components of Linseed Oil Paint Films. Stud Conserv 48:111-135. doi: 10.1179/sic.2003.48.2.111

[57] Rossi M, Alamprese C, Ratti S (2007) Tocopherols and tocotrienols as free radical-scavengers in refined vegetable oils and their stability during deep-fat frying. Food Chem 102:812-817. doi: 10.1016/j.foodchem.2006.06.016

[58] Webster RD (2007) New Insights into the Oxidative Electrochemistry of Vitamin E. Accounts Chem Res 40:251-257. doi: 10.1021/ar068182a

[59] Malyzsko J, Karbarz M (2006) Electrochemical oxidation of trolox and α-tocopherol in acetic acid: A comparative study. J Electroanal Chem 595:136-144. doi: 10.1016/j.jelechem.2006.07.018

[60] Madani A, Nessark B, Boukherroub R, Chehimi MM (2011) Preparation and electrochemical behaviour of PPy–CdS composite films. J Electroanal Chem 650:176-181. doi: 10.1016/j.jelechem.2010.10.017

[61] Derrick MR, Stulik DC, Landry MJ (1999) Infrared Spectroscopy in Conservation Science. Getty Conservation Institute, Los Angeles

[62] van der Weerd J, van Loon A, Boon JJ (2005) FTIR studies of the effects of pigments on the aging of oil. Stud Conserv 50:3-22. doi: 10.2307/25487713

[63] Kong J, Yu S (2007) Fourier Transform Infrared Spectroscopic Analysis of Protein Secondary Structures. Acta Bioch Bioph Sin 39:549-559. doi: 10.1111/j.1745-7270.2007.00320.x

[64] Haris PI, Severcan F (1999) FTIR spectroscopic characterization of protein structure in aqueous and non-aqueous media. J Mol Catal B-Enzym 7:207-221. doi: 10.1016/s1381-1177(99)00030-2

[65] Furlan PY, Scott SA, Peaslee MH (2007) FTIR-ATR Study of pH effects on egg albumin secondary structure. Spectrosc Lett 40:475-482. doi: 10.1080/00387010701295950

[66] Dong A, Huang P, Caughey WS (1990) Protein secondary structures in water from second-derivative amide I infrared spectra. Biochemistry-US 29:3303-3308. doi: 10.1021/bi00465a022

[67] Rajkhowa R, Hu X, Tsuzuki T, Kaplan DL, Wang X (2012) Structure and biodegradation mechanism of milled *B. mori* silk particles. Biomacromolecules 13:2503-2512. doi: 10.1021/bm300736m

[68] Anton M (2013) Egg yolk: structures, functionalities and processes. J Sci Food Agr 93:2871–2880. doi: 10.1002/jsfa.6247

[69] Hevonoja T, Pentikäinen MO, Hyvönen MT, Kovanen PT, Ala-Korpela M (2000) Structure of low density lipoprotein (LDL) particles: Basis for understanding molecular changes in modified LDL. Biochim Biophys Acta 1488:189-210. doi: 10.1016/s1388-1981(00)00123-2

[70] Kumpula LS, Kumpula JM, Taskinen MR, Jauhiainen M, Kaski K, Ala-Korpela M (2008) Reconsideration of hydrophobic lipid distributions in lipoprotein particles. Chem Phys Lipids 155:57–62 and references therein. doi: 10.1016/j.chemphyslip.2008.06.003

[71] Schneider H, Morrod RS, Colvin JR, Tattrie NH (1973) The lipid core model of lipoproteins. Chem Phys Lipids 10:328-353. doi: 10.1016/0009-3084(73)90058-3

[72] Doménech-Carbó MT, Osete-Cortina L, de la Cruz-Cañizares J, Bolívar-Galiano F, Romero-Noguera J, Martín-Sánchez I, Fernández-Vivas MA (2006) Study of the microbiodegradation of terpenoid resin-based varnishes from easel painting using pirolisis-gas chromatography-mass spectrometry and gas chromatography-mass spectrometry. Anal Bioanal Chem 385:1265-1280. doi: 10.1007/s00216-006-0582-3

Table 1. Band area ratios of the inoculated egg yolk tempera and egg-oil emulsion paint films.

				Fungi				Bacteria	
Band area ratio									
Egg Yolk	**Blank**	**Ac**	**An**	**Mr**	**Pc**	**Tp**	**Ao**	**Ba**	**Sc**
C=O/Amide I	0.18	0.14	0.14	0.09	0.16	0.15	0.12	0.10	0.09
C=O/Amide II	0.33	0.28	0.27	0.17	0.29	0.29	0.24	0.19	0.16
Emulsion	**Blank**	**Ac**	**An**	**Mr**	**Pc**	**Tp**	**Ao**	**Ba**	**Sc**
C=O/Amide I	0.48	0.27	0.34	0.17	0.34	0.47	0.16	0.09	0.16
C=O/Amide II	0.76	0.48	0.53	0.29	0.55	0.75	0.29	0.15	0.27

Table 2. Summary of the electrochemical processes involved in biodeterioration of reconstructed EG and EO paint films.

Process	System	Description
C_1	CdS	Reduction of bare CdS grains to Cd metal (Eq. (1))
C_3	EG@Blank	Reduction of CdS surface complexes with proteins mainly in β-sheet conformation (Eq(2))
C_4	EO@Blank	Reduction of Cd(II)-carboxylates with fatty acids (Eq. (3))
C_5	EG @fungi EG @bacteria	Reduction of CdS surface complexes with proteins mainly in random coil conformation (Eq(2))

Figures

Figure 1. Secondary electron images obtained with FESEM of: a) the cross-section of a reconstructed egg tempera paint film (EG) and b) the cross-section of a reconstructed egg –oil emulsion paint film (EO).

Figure 2. Secondary electron images obtained with FESEM on the surface of a reconstructed egg tempera paint film inoculated by *Aspergillus niger* (EG@An).

Figure 3. Cyclic voltammograms, after semi-derivative convolution of: a) a microparticulate deposits of CdS; b) sample of un-inoculated egg tempera paint film (EG@Blank); c) sample of un-inoculated egg-oil emulsion paint film (EO@Blank) attached to graphite bar immersed into 0.25 M sodium acetate buffer, pH 4,75. Potential scan rate 50 mV s^{-1}.

Figure 4. SECM map colors of a,b) sample of un-inoculated egg tempera paint film (EG@Blank) and c,d) sample of un-inoculated egg-oil emulsion paint film (EO@Blank) attached to a graphite plate in contact with electrode in contact with 5.0 mM $K_4Fe(CN)_6$ solution in 0.25 M HAc/NaAc (pH 4.75) before (a,c) and after (b,d) application of a potential input of –1.0 V during 2 min. E_T = +0.30 V.

Figure 5. Topographic AFM images of a un-inoculated egg tempera paint film EG@Blank on a graphite plate in contact with 0.25 M sodium acetate buffer, pH 4,75, a,b) before, and c,d) after application of a potential step of -1.0 V during 5 min.

Figure 6. Cyclic voltammograms, after semi-derivative convolution, for graphite electrodes modified with egg-oil emulsion paint film (EO) immersed into 0.25 M sodium acetate buffer, pH 4,75 after incubation with: a) *Aspergillus niger* (EO@An); b) *Acremonium crhysogenum* (EO@Ac); c) *Bacillus amyloliquefaciens* (EO@Ba); d) *Arthrobacter oxydans* (EO@Ao). Potential scan rate 50 mV s^{-1}.

Figure 7. Cyclic voltammograms, after semi-derivative convolution, for graphite electrodes modified with egg tempera paint film immersed into 0.25 M sodium acetate

buffer (EG), pH 4,75 after incubation with: a) the fungus *Trichoderma pseodukoningii* (EG@Tp); b) the bacterium *Streptomyces cellulofans* (EG@Sc). Potential scan rate 50 mV s^{-1}.

Figure 8. Linear scan voltammograms, after semi-derivative convolution, for: a) pure cadmium yellow b) pure egg yolk, c) EG@Blank paint film d) EG@An paint film deposited on graphite in contact with 0.25 M sodium acetate buffer, pH 4,75. Potential scan initiated at 0.0 V in the positive direction; potential scan rate 50 mV s^{-1}.

Figure 9. Linear scan voltammograms, after semi-derivative convolution, for films of: a) pure egg + linseed oil emulsion b) EO@Blank, c) EO@Ba and d) EO@An, deposited on graphite in contact with 0.25 M sodium acetate buffer, pH 4,75. Potential scan initiated at –0.40 V in the positive direction; potential scan rate 50 mV s^{-1}.

Figure 10. IR absorption spectra of EG@Blank and EO@Blank reconstructed paint films. Spectra are presented in staked mode.

Figure 11. a) Detail of the deconvoluted amide I band obtained from the series of reconstructed egg tempera paint films. b) Detail of the deconvoluted amide I band obtained from the series of reconstructed egg-oil emulsion paint films. α: helical conformations; β-1: intramolecular β-sheet; β-2: intermolecular β-sheet; rc: random coil; t: turns.

Figure 1.

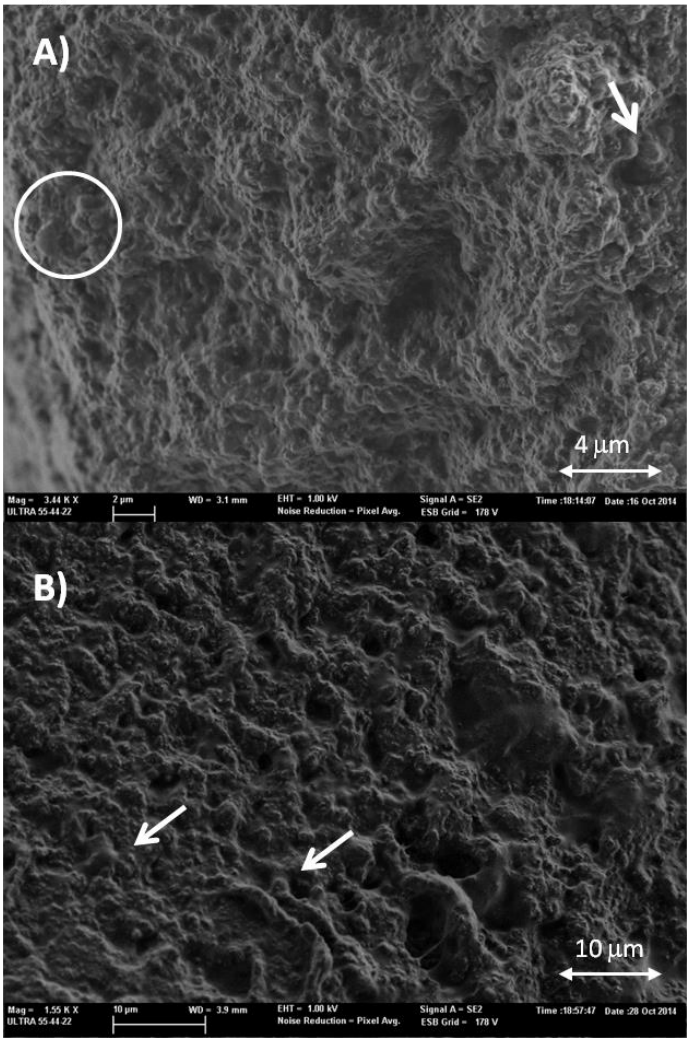
A)
4 µm
Mag = 3.44 K X
ULTRA 55-44-22
2 µm
WD = 3.1 mm
EHT = 1.00 kV
Noise Reduction = Pixel Avg.
Signal A = SE2
ESB Grid = 178 V
Time :18:14:07 Date :16 Oct 2014
B)
10 µm
Mag = 1.55 K X
ULTRA 55-44-22
10 µm
WD = 3.9 mm
EHT = 1.00 kV
Noise Reduction = Pixel Avg.
Signal A = SE2
ESB Grid = 178 V
Time :18:57:47 Date :28 Oct 2014

Figure 2.

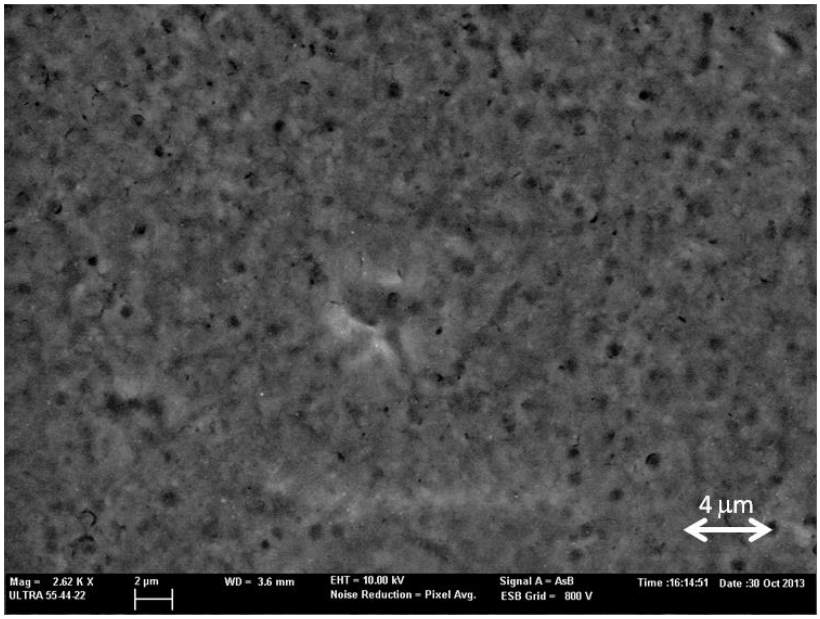
4 µm
Mag = 2.62 K X
ULTRA 55-44-22
2 µm
WD = 3.6 mm
EHT = 10.00 kV
Noise Reduction = Pixel Avg.
Signal A = AsB
ESB Grid = 800 V
Time :16:14:51 Date :30 Oct 2013

Figure 3

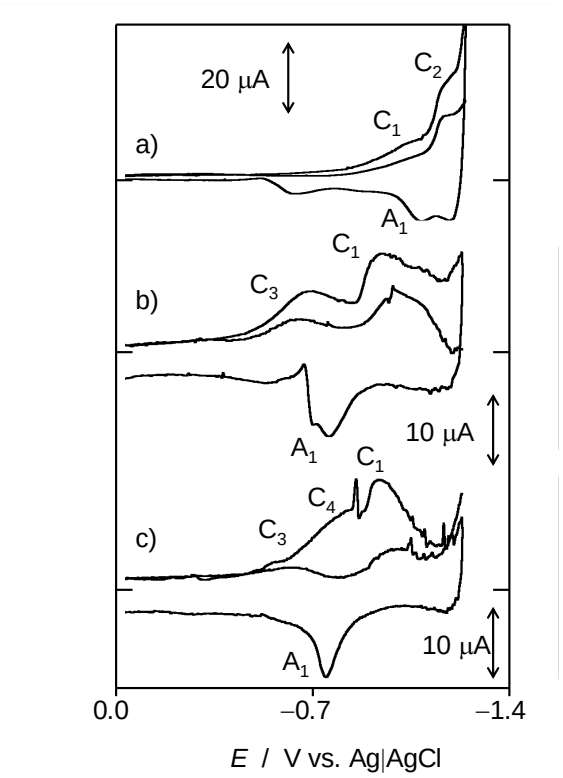
20 μA
C2
C1
a)
A1
C1
C3
b)
10 μA
A1
C1
C4
C3
c)
10 μA
A1
0.0
–0.7
–1.4
E / V vs. Ag|AgCl

Figure 4

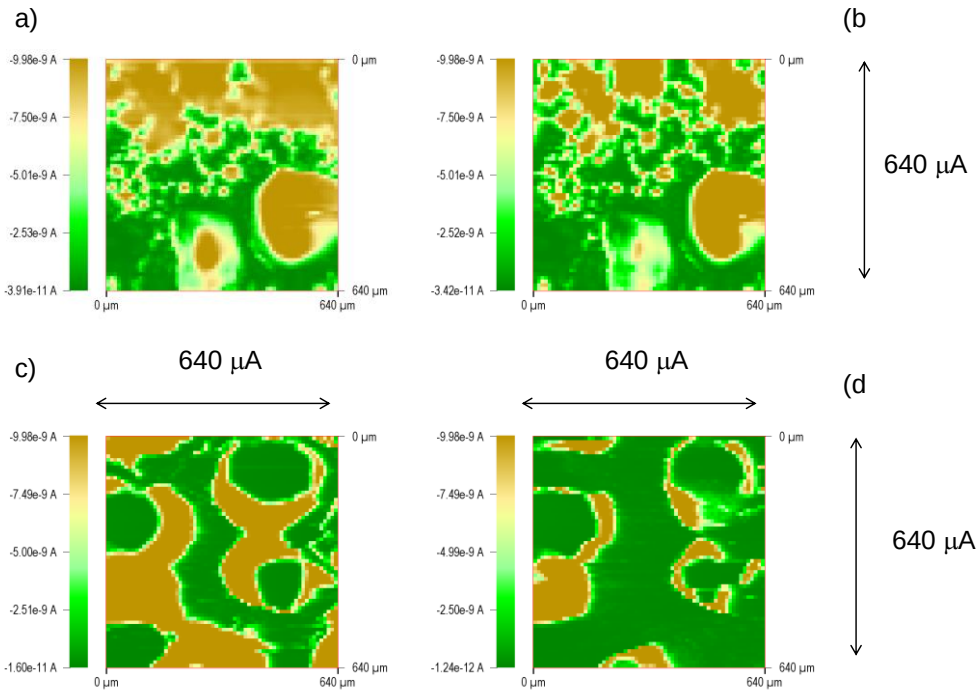
a)
-9.98e-9 A
-7.50e-9 A
-5.01e-9 A
-2.53e-9 A
-3.91e-11 A
0 µm
640 µm
0 µm
640 µm
(b
-9.98e-9 A
-7.50e-9 A
-5.01e-9 A
-2.52e-9 A
-3.42e-11 A
0 µm
640 µm
0 µm
640 µm
640 µA
c)
640 µA
-9.98e-9 A
-7.49e-9 A
-5.00e-9 A
-2.51e-9 A
-1.60e-11 A
0 µm
640 µm
0 µm
640 µm
640 µA
-9.98e-9 A
-7.49e-9 A
-4.99e-9 A
-2.50e-9 A
-1.24e-12 A
0 µm
640 µm
0 µm
640 µm
(d
640 µA

Figure 5

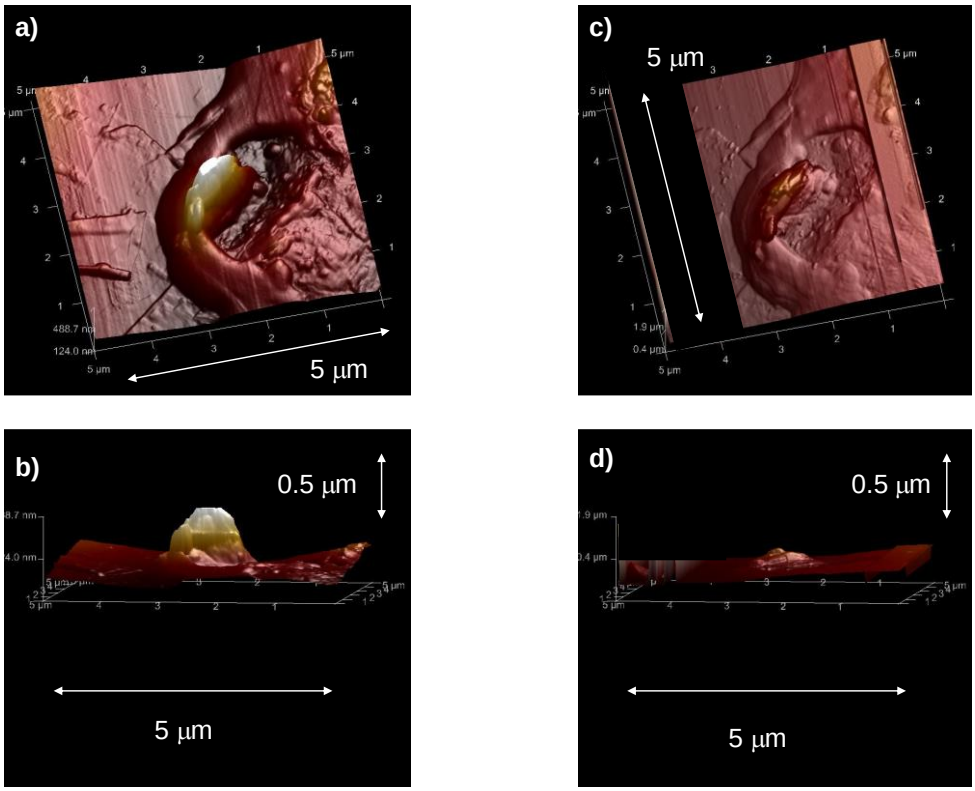

Figure 6

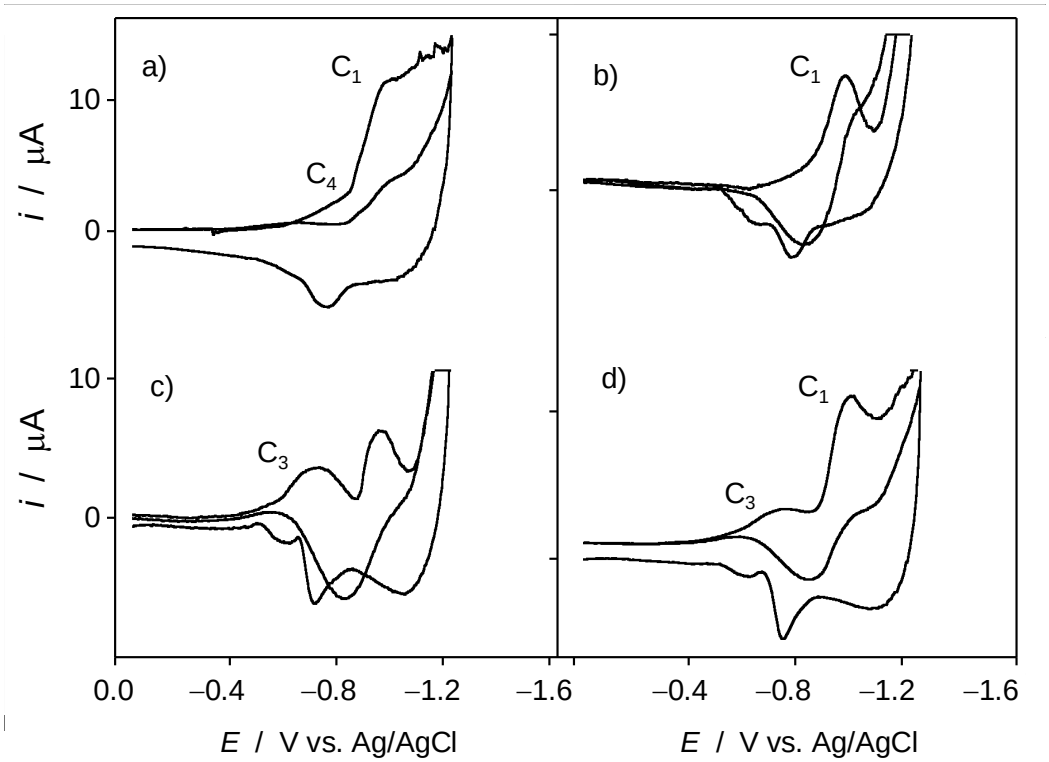

Figure 7

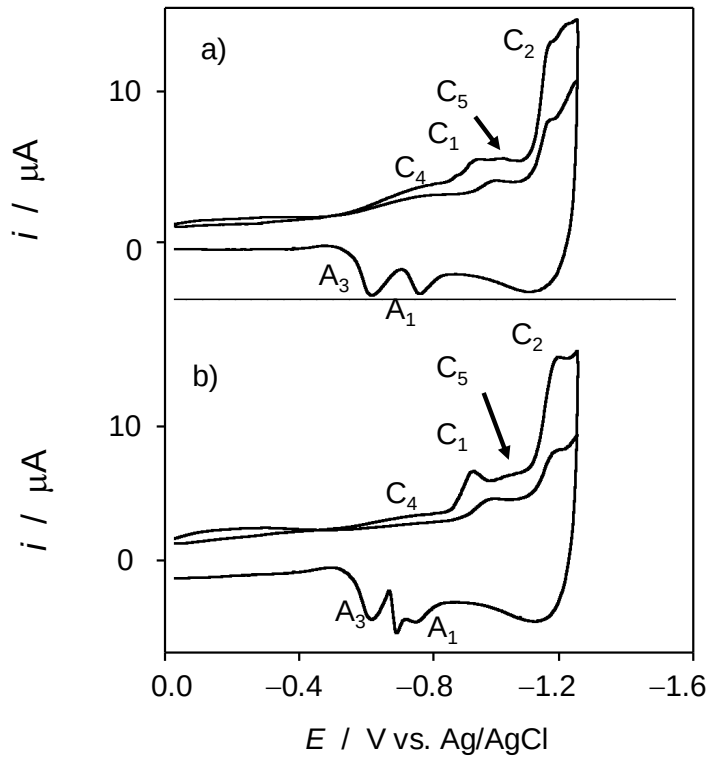

Figure 8

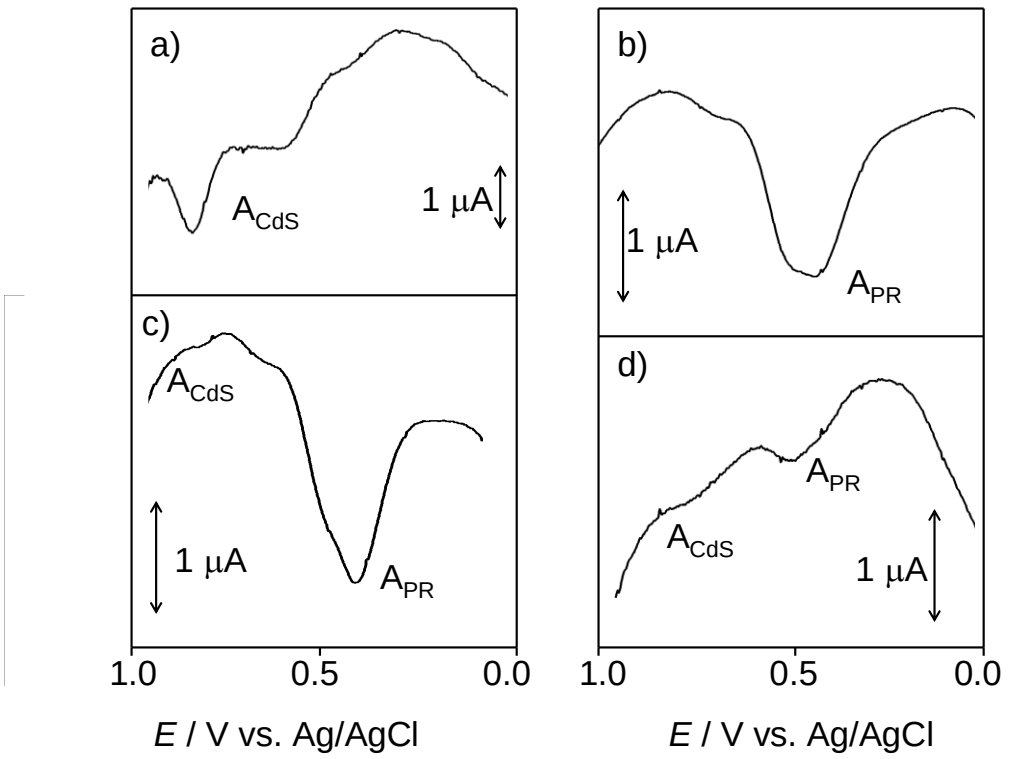
a)
A_{CdS}
1 μA
b)
1 μA
A_{PR}
c)
A_{CdS}
1 μA
A_{PR}
d)
A_{PR}
A_{CdS}
1 μA
1.0
0.5
0.0
1.0
0.5
0.0
E / V vs. Ag/AgCl
E / V vs. Ag/AgCl

Figure 9

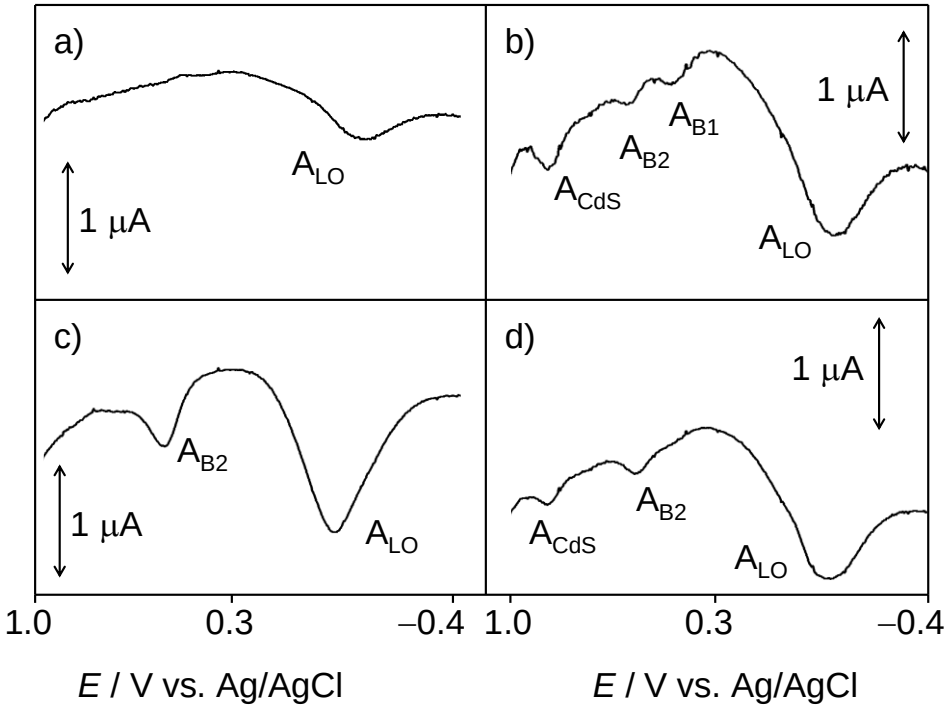
a)
A_{LO}
1 μA
b)
1 μA
A_{B1}
A_{B2}
A_{CdS}
A_{LO}
c)
A_{B2}
1 μA
A_{LO}
d)
1 μA
A_{B2}
A_{CdS}
A_{LO}
1.0
0.3
–0.4
1.0
0.3
–0.4
E / V vs. Ag/AgCl
E / V vs. Ag/AgCl

Figure 10

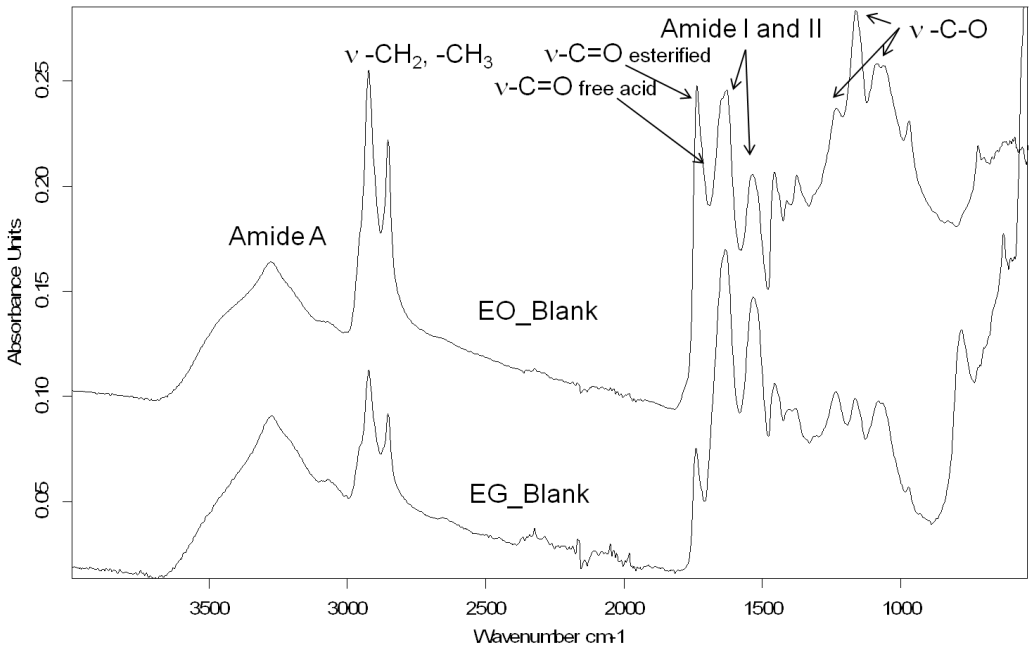
Amide I and II
ν -C-O
ν -CH2, -CH3
ν-C=O esterified
ν-C=O free acid
Amide A
EO_Blank
EG_Blank
Absorbance Units
0.05
0.10
0.15
0.20
0.25
3500
3000
2500
2000
1500
1000
Wavenumber cm-1

Figure 11

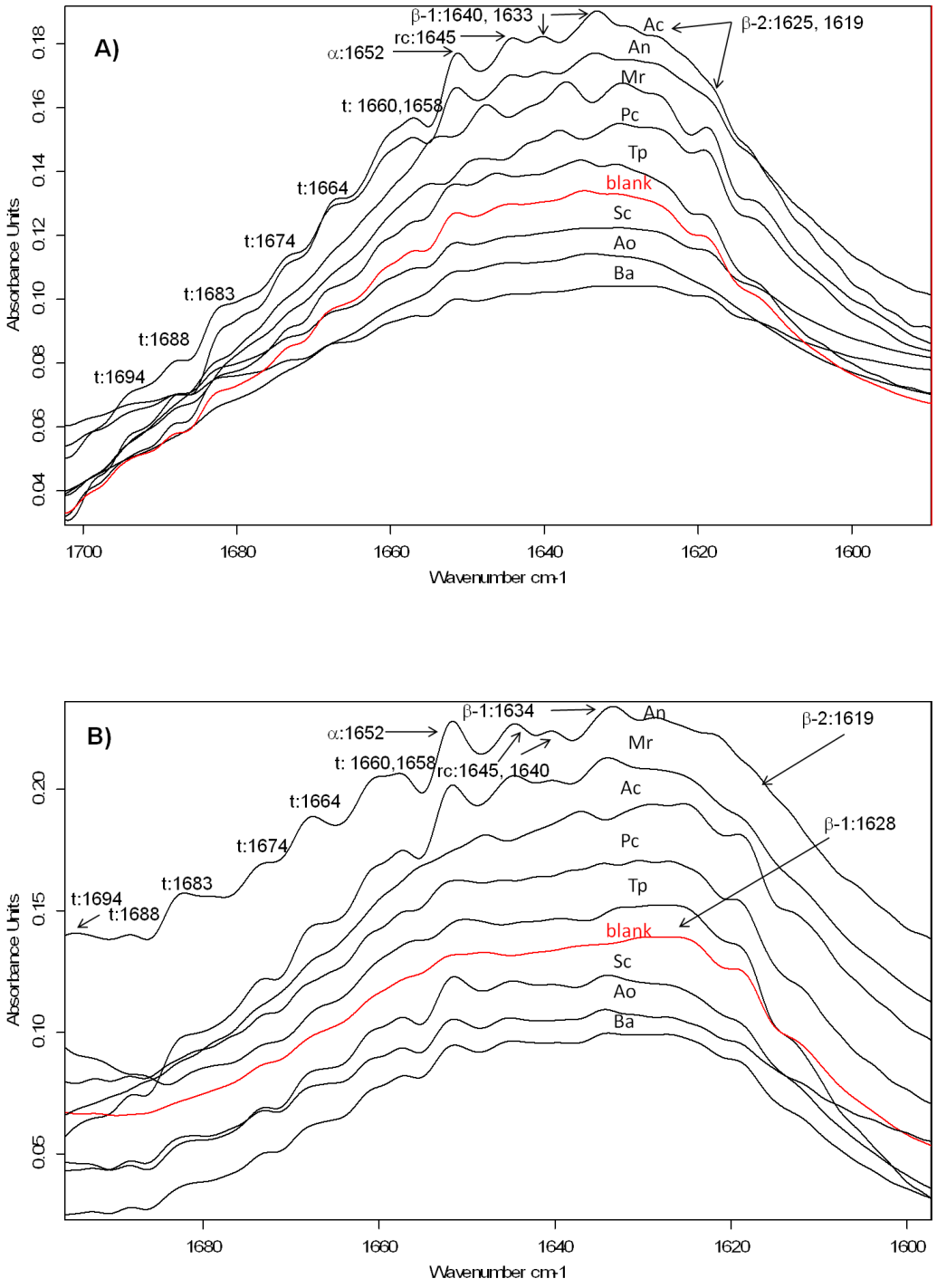
A)
β-1:1640, 1633
rc:1645
α:1652
t: 1660,1658
t:1664
t:1674
t:1683
t:1688
t:1694
Ac
An
Mr
Pc
Tp
blank
Sc
Ao
Ba
β-2:1625, 1619
Absorbance Units
0.04
0.06
0.08
0.10
0.12
0.14
0.16
0.18
1700
1680
1660
1640
1620
1600
Wavenumber cm-1
B)
β-1:1634
α:1652
t: 1660,1658
rc:1645, 1640
t:1664
t:1674
t:1683
t:1694
t:1688
An
Mr
Ac
Pc
Tp
blank
Sc
Ao
Ba
β-2:1619
β-1:1628
Absorbance Units
0.05
0.10
0.15
0.20
1680
1660
1640
1620
1600
Wavenumber cm-1

Graphical Abstract

Click here to download Graphical Abstract
CdSebiodeterElectrochemCoverFigure.ppt